Environ. Sci. Technol. **1998**, *32,* 956−965

Rock−Water Interactions Controlling Zinc, Cadmium, and Lead Concentrations in Surface Waters and Sediments, U.S. Tri-State Mining District. 2. Geochemical Interpretation

SUSAN A. CARROLL,*,† PEGGY A. O'DAY,‡ AND MIKE PIECHOWSKI§

Earth and Environmental Sciences Directorate, Lawrence Livermore National Laboratory, Livermore, California 94550, Department of Geology, Arizona State University, Tempe, Arizona 85287-1404, and Department of Geological Sciences, University of Missouri, Columbia, Missouri 65211

We have studied principle rock−water interactions that control trace metal concentrations in a complex geochemical environment containing multiple contaminants and multiple solid phases by combining kinetic and thermodynamic evaluation of the water chemistry with spectroscopic analyses of the sediments. This approach allows the number of geochemical reactions needed to model and predict trace metal mobility over a range of natural settings to be greatly constrained. In the U.S. Tri-State Mining District (Kansas−Missouri−Oklahoma) the most important geochemical interactions are degassing of CO_2(g)-rich waters; the short-term uptake and release kinetics of zinc, cadmium, and lead; competition between iron oxyhydroxides and carbonates for zinc, cadmium, and lead; and catalysis of sulfide dissolution by iron in near-neutral waters. In our field study, degassing of CO_2(g) waters is responsible for the range of pH measured at each site over the 1-year field study. Trace metal release and uptake kinetics by iron oxyhydroxides and carbonates are driven by changes in pH. Aqueous metal concentrations and pH of pond water and streamwater in contact with high-iron sediments suggest that oxidation−reduction reactions involving iron accelerate sphalerite dissolution kinetics in near-neutral waters. This study clearly shows that zinc is preferentially partitioned into secondary zinc hydroxide or iron oxyhydroxide, but in the same sediments cadmium is not. Cadmium is the most mobile element because it dissolves from sulfide and is taken up by calcite only in waters with pH > 7. Lead is taken up by carbonate or iron oxyhydroxide and is extremely insoluble in these near-neutral waters. To accurately predict trace metal mobility in complex environments, laboratory studies are needed to quantify competition effects among multiple metals for carbonate and iron oxyhydroxide phases and to quantify reaction rates of metal release and uptake from sulfides and secondary phases in the presence of dissolved iron.

Introduction

A major source of trace metal contamination of surface and groundwaters is due to mining activities that expose unstable sulfides to oxygen-rich waters. These environments are geochemically complex with multiple contaminants and multiple solid phases that impact the partitioning of metals between more mobile waters and less mobile sediments. Important geochemical processes include dissolution and precipitation kinetics, sorption to mineral surfaces, and chemical behavior of major elements such as carbon, iron, silica, and sulfur.

The geochemical understanding of trace metals in the earth's near-surface environment has been advanced by numerous well-controlled laboratory investigations. The motivation behind these experiments is to study simple systems to better understand more complex natural or contaminated systems. Sorption studies show that trace metals are preferentially removed from solutions below pure phase solubility by calcite and iron oxyhydroxide (*2, 3*). Recent X-ray absorption spectroscopy studies have further advanced the geochemical understanding of trace metal uptake reactions by determining the speciation and bonding of these elements at the solid−solution interface (see reviews in refs 4 and 5). However, model studies often fail to address the competition between different substrates for trace metals and the nonequilibrium chemistry of surface and groundwaters.

The objective of this study is to combine aqueous and sediment geochemical analyses to determine the rock−water interactions that control trace metal distribution in a mine drainage system. We chose to study the partitioning of zinc, cadmium, and lead between the surface waters and top 5 cm of sediments in two small streams in the U.S. Tri-State Mining District. Our geochemical interpretations are based in part on atomic level structural characterization of zinc, cadmium, and lead in these sediments using X-ray absorption spectroscopy and other microscopic techniques (*1*). We discuss the importance of kinetic processes and the competition of carbonates and iron oxyhydroxides for trace metals in a complex contaminated environment.

Field Sampling and Analysis. The U.S. Tri-State Mining District (Kansas−Missouri−Oklahoma), a Mississippi Valley type ore deposit, is characterized by zinc and lead sulfide mineralization associated with a chert and carbonate host rock (*6, 7*). Commercial mining spanned the 1840s to the late 1960s; during peak production in the 1920s, about 352 000 t of zinc and 92 000 t of lead were produced. The remaining tailings piles consist of mostly chert, a few weight percent calcite and dolomite, as well as residual sphalerite, galena, pyrite, and marcasite. The underground mines are filled with water that discharges into the local surface waters. The primary source of the trace metals is sphalerite for zinc and cadmium (0.5 wt %) and galena for lead.

Surface waters and sediments were sampled bimonthly at two small streams within the U.S. Tri-State Mining District from August 1991 to July 1992 (Figure 1). Mineral Branch drains a large portion of the Webb City Mining Field from south to north. Four of the five Mineral Branch sample locations are within the stream channel, and one is a pond in the tailings about 0.2 km west of the stream channel (site 3). Site 5 is the spring source of Mineral Branch. Tar Creek drains the Eagle-Picher Mining Field from north to south. Of the 13 sites, eight are located on the Tar Creek channel, two are located on Lytle Creek (a major tributary), and three are

* To whom correspondence should be addressed. Voice: (510) 423-5694; fax: (510) 422-0208; e-mail: carroll6@llnl.gov.
† Lawrence Livermore National Laboratory.
‡ Arizona State University.
§ University of Missouri.

S0013-936X(97)00452-5 CCC: $15.00
Published on Web 02/28/1998

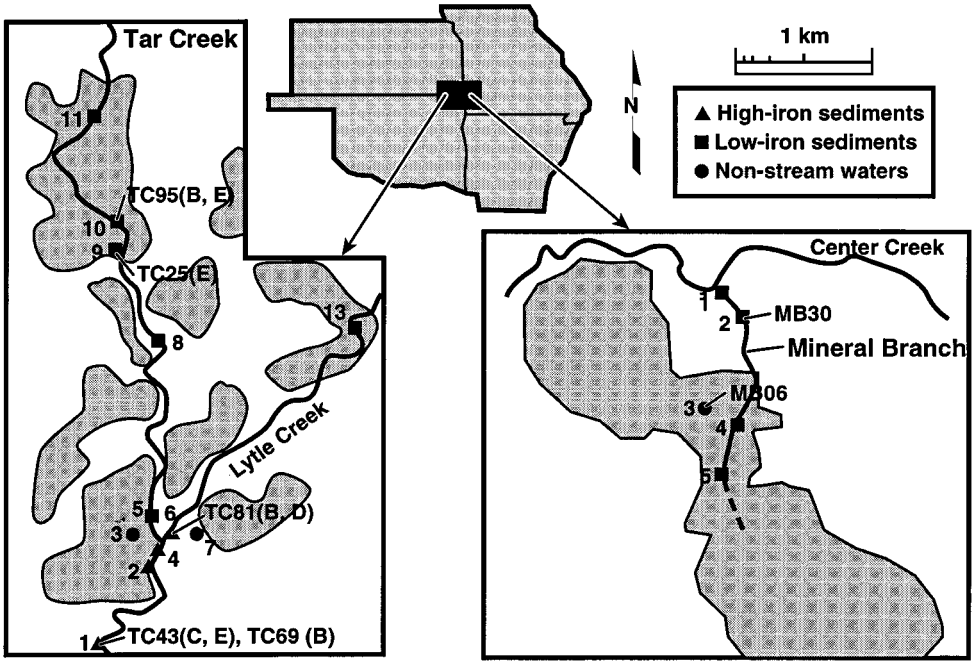

FIGURE 1. Tar Creek and Mineral Branch sample locations in the U.S. Tri-State Mining District. Shaded areas represent tailings piles. Sediments analyzed with XAS are labeled (*1*).

located either in ponded areas or in minor tributaries. There is an abundance of visible iron oxyhydroxide at the intersection of Tar Creek and Lytle Creek. No visible iron oxyhydroxide is present upstream from this intersection or in the Mineral Branch waters.

During sample collection, the following protocol was carried out at each site. (a) pH and temperature of the streams were measured using a portable pH meter with automatic temperature correction. The pH electrode was standardized a minimum of twice daily with pH 4 and pH 7 buffers. (b) Aqueous samples were collected with a wide-mouthed 500 mL glass bottle. Samples were collected along a transect line stretched across the stream perpendicular to the current. A sample churn (similar to the type used by the USGS) was used to homogenize water samples. Before each aqueous sample was collected, the collection bottle and the churn were rinsed with streamwater and emptied downstream. (c) Solid samples were gathered at both sides and the center of the site, conditions permitting. The sample bottle was usually used as a scoop to collect sediment. The bottle was filled underwater by scooping sediments into it until full. Solid sample bottles were filled with water from the location where they were collected. (d) Two aqueous samples were filtered for a field alkalinity titration and further analysis with a peristaltic pump, a 142 mm filter assembly, and Norprene tubing. All wetted surfaces of the pump and filter were constructed of nonmetallic parts. Filter pore size was usually 0.10 μm (0.22 μm filters were used for six samples, and no differences in the aqueous analyses were noted). The filter assembly was flushed with filtrate before sample collection, and acid-washed polypropolyene sample bottles were rinsed twice with filtered sample before sample collection. After each use, the filter was discarded; the entire filter assembly, including the pump tubing, was cleaned and rinsed thoroughly with distilled water. (e) Alkalinity was determined by titration with a strong acid to pH 4.5.

Laboratory Analysis. The sediments were processed to dry powders for all analyses. The sediment samples were rinsed out of their sample bottles with a bicarbonate solution buffered at the sample pH measured at time of collection to minimize additional reactions during processing. After being rinsed, the samples were dried in an oven at 60 °C and then sieved into five size fractions: A, > 1.0 mm; B, 0.63−1.0 mm; C, 0.32−0.63 mm; D, 0.14−0.32 mm; and E, < 0.14 mm. X-ray diffraction (XRD) and X-ray absorption spectroscopy (XAS) analyses are described in O'Day et al. (*1*).

Total metal concentrations of the sediment and aqueous samples were determined by inductively coupled plasma atomic emission spectrometry (ICP-AES). Detection limits for Al = 60, Ba = 10, Ca = 2, Cd = 10, Fe = 10, K = 100, Mg = 3, Mn = 3, Na 200, Pb = 30, Si =30, Sr = 10, and Zn = 10 ppb. Most of the aqueous samples were analyzed directly with no pretreatment. Some Tar Creek aqueous samples precipitated an iron solid before analysis. These samples were acidified with trace metal grade HNO_3 to dissolve the precipitate completely. A $LiBO_3$ flux and trace metal grade HNO_3 were used to completely digest the sediments prior to ICP-AES analysis.

Geochemical Modeling. The aqueous data were analyzed with the Geochemist's Workbench geochemical code (*8*) and SUPCRT92 database (*9*) modified to include zinc, cadmium, and lead carbonate and zinc and cadmium hydroxide phases (Table 1). For these calculations, we used the field pH, field temperature, field alkalinity, and total measured metal concentrations. The field alkalinity is assumed to be equal to the bicarbonate concentration. The solution was charge balanced by adjusting the sulfate concentration, because it was not measured in the field and was likely to be a major sulfur species. Calculated sulfate concentrations are on the order of 2 mM, which agrees with sulfate concentrations in other mine drainage field studies (*10*−*13*). No differences in the most stable mineral assemblages were observed when the same solutions were charge balanced by adjusting the Cl^- concentration.

Results

Aqueous Geochemistry. We divide the sample locations into three geochemical groups: (a) Streamwaters in contact with low iron sediments (<10 wt % Fe) consisting of quartz and lesser amounts of calcite, dolomite, and sphalerite. Mineral Branch sites 1, 2, 4, and 5 and Tar Creek sites upstream from Lytle Creek are in this group. (b) Streamwaters in contact with high-iron sediments, consisting of amorphous iron

TABLE 1. Thermodynamic Data

	log K (25 °C)	ref
$CaCO_3$ (calcite) = $Ca^{2+} + CO_3^{2-}$	−8.48	42
$CaMg(CO_3)_2$ (dolomite) = $Ca^{2+} + Mg^{2+} + 2CO_3^{2-}$	−18.14	42
$CaSO_4 \cdot 2H_2O$(gypsum) = $Ca^{2+} + SO_4^{2-} + 2H_2O$	−4.48	43
$Cd^{2+} + H_2O = CdOH^+ + H^+$	−10.08	44
$Cd^{2+} + 2H_2O = Cd(OH)_2^0 + 2H^+$	−20.34	44
$Cd^{2+} + 3H_2O = Cd(OH)_3^- + 3H^+$	−33.29	44
$Cd^{2+} + 4H_2O = Cd(OH)_4^{2-} + 4H^+$	−47.33	44
$Cd^{2+} + CO_3^{2-} = CdCO_3^0$	3.00	30
$Cd^{2+} + 2CO_3^{2-} = Cd(CO_3)_2^{2-}$	6.40	30
$Cd^{2+} + CO_3^{2-} + H^+ = CdHCO_3^+$	11.83	30
$Cd^{2+} + SO_4^{2-} = Cd\ SO_4^0$	−0.003	45
$Cd(OH)_2$ (β) + $2H^+ = Cd^{2+} + 2H_2O$	13.74	44
$CdSO_4$ (solid) = $Cd^{2+} + SO_4^{2-}$	−0.11	45
$CdCO_3$ (otavite) = $Cd^{2+} + CO_3^{2-}$	−12.1	30
CdO (monteponite) + $2H^+ = Cd^{2+} + H_2O$	15.1	46
Fe_2O_3 (hematite) + $6\ H^+ = 2Fe^{3+} + 3H_2O$	0.11	42
FeOOH (goethite) + $3H^+ = Fe^{3+} + 2H_2O$	0.53	43
$Fe(OH)_3$ (am) + $3H^+ = Fe^{3+} + 3H_2O$	5.66	45
$Pb^{2+} + H_2O = PbOH^+ + H^+$	−7.7	47
$Pb^{2+} + 2H_2O = Pb(OH)_2 + 2H^+$	−17.09	47
$Pb^{2+} + 3H_2O = Pb(OH)_3^- + 3H^+$	−28.09	47
$Pb^{2+} + CO_3^{2-} = PbCO_3$	6.58	48[a]
$Pb^{2+} + 2CO_3^{2-} = Pb(CO_3)_2^{2-}$	9.40	48[a]
$PbCO_3$ (cerussite) = $Pb^{2+} + CO_3^{2-}$	−13.54	9
$Pb_3(CO_3)_2(OH)_2$ (hydrocerussite) + $2H^+ = 2CO_3^{2-} + 3Pb^{2+} + 2H_2O$	−18.81	47
$PbSO_4$ (anglesite) = $Pb^{2+} + SO_4^{2-}$	−7.85	42
SiO_2 (quartz) = SiO_2(aq)	−4.0	42
SiO_2 (am) = SiO_2(aq)	−2.71	42
$Zn^{2+} + H_2O = ZnOH^+ + H^+$	−8.96	49
$Zn^{2+} + 2H_2O = Zn(OH)_2^0 + 2H^+$	−17.33	45
$Zn^{2+} + 3H_2O = Zn(OH)_3^- + 3H^+$	−28.83	45
$Zn^{2+} + 4H_2O = Zn(OH)_4^- + 4H^+$	−41.61	45
$Zn^{2+} + CO_3^{2-} + H^+ = ZnHCO_3^+$	11.75	49
$Zn^{2+} + CO_3^{2-} = ZnCO_3^0$	3.9	21
$Zn^{2+} + SO_4^{2-} = Zn\ SO_4^0$	−2.31	45
$Zn(OH)_2$ (β) + $2H^+ = Zn^{2+} + 2H_2O$	11.93	45
$Zn(OH)_2$ (ϵ) + $2H^+ = Zn^{2+} + 2H_2O$	11.66	45
$Zn(OH)_2$ (γ) + $2H^+ = Zn^{2+} + 2H_2O$	11.88	45
$ZnSO_4$ (solid) = $Zn^{2+} + SO_4^{2-}$	3.55	45
$ZnCO_3$ (smithsonite) = $Zn^{2+} + CO_3^{2-}$	−9.87	9
$Zn_5(OH)_6(CO_3)_2$ (hydrozincite) + $6\ H^+ = 5\ Zn^{2+} + 2CO_3^{2-} + 6H_2O$	9.65	50

[a] Experimental values extrapolated to $I = 0$.

TABLE 2. Mineral Branch and Tar Creek Water Chemistry[a]

	Mineral Branch			Tar Creek		
	max	median	min	max	median	min
pH	8.5	7.0	5.5	7.8	6.7	3.8
T (°C)	30.7	17.0	3.4	33.2	20.1	0.9
Alk. (ppm HCO_3^-)	219.1	149.7	15.5	289.3	122.7	0.0
SO_4^{2-} (ppm)	781	403.5	72.6	1537	492.0	20.0
Major Elements (ppm)						
Al				1.20	0.00	
Ca	343	185.5	25.0	616.0	210.0	16.0
Fe	0.044	0.000		176.9	0.00	
K	3.40	1.10	0.40	9.3	2.9	0.42
Mg	5.59	4.47	76.0	127.3	21.0	3.35
Mn	1.61	0.12		12	0.49	
Na	6.25	5.86	0.65	46.4	8.15	2.55
Si	6.68	4.69	2.59	12.4	5.07	1.75
Trace Metals (ppm)						
Ba	0.12	0.02		9.39	0.03	
Cd	0.44	0.03		2.1	0.00	
Pb	0.15	0.00		31.4	0.00	
Sr	0.24	0.13	0.04	0.89	0.25	0.07
Zn	43.4	2.09	0.01	725	7.70	

[a] Maximum, median, and minimum values are reported from 74 mineral branch and 79 tar creek water analyses.

TABLE 3. Mineral Branch and Tar Creek Sediment Chemistry[a]

	Mineral Branch			Tar Creek		
	max	median	min	max	median	min
Major Elements (wt %)						
Al	9.88	2.79	0.19	7.89	0.95	0.30
Ca	33.10	.62	0.02	8.72	1.56	0.14
Fe	8.47	3.17	0.37	52.2	3.59	0.51
K	2.29	0.72	0.16	2.85	0.28	
Mg	0.53	0.20	0.02	2.43	0.47	0.04
Mn	1.82	0.06		1.32	0.043	
Na	0.72	0.14		0.37	0.08	
Si	53.23	34.23	0.04	40.73	32.25	1.31
Zn	9.62	1.50	0.05	8.53	1.76	0.02
Trace Metals (ppm)						
Ba	833	273		6339	75	
Cd	813	76		386	58	
Pb	13 183	1402		4589	433	
Sr	90	44		153	24	

[a] Maximum, median, and minimum values are reported from 55 mineral branch and 117 tar creek stream sediment samples.

oxyhydroxide or poorly crystalline goethite (10−65 wt % Fe), quartz, calcite, dolomite, and sphalerite. Lytle Creek site 6 and Tar Creek sites downstream from Lytle Creek are in this group. (c) Waters in ponded areas near the streams. Mineral Branch site 3 and Tar Creek sites 3, 7, and 12 are in this group.

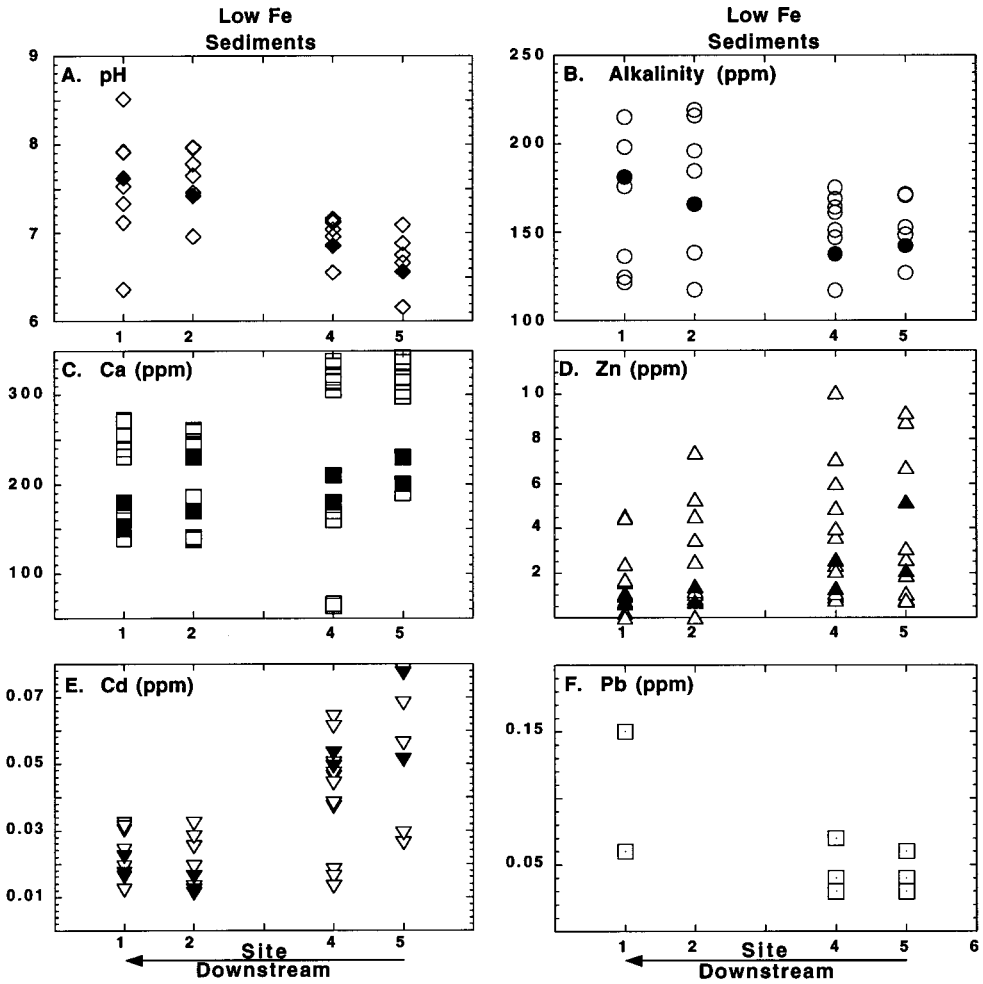

FIGURE 2. Mineral Branch pH, alkalinity, and aqueous Zn, Cd, and Pb concentrations measured at each sampling site over the 1-year sampling period; solid symbols represent one sampling trip. All waters are in contact with low-iron sediments.

Tables 2 and 3 report the range of water and sediment compositions in Mineral Branch and Tar Creek over the 1-year sampling period. The major aqueous components are bicarbonate, sulfate, calcium, magnesium, and silica and reflect inputs from the carbonate geology, sulfide ore, and chert tailings. Zinc concentrations are about 3 orders of magnitude higher than cadmium and lead. Water pH varies from 3.8 to 8.5.

Figures 2−4 show the significant spatial and temporal variation of pH, alkalinity, calcium, zinc, cadmium, and lead concentrations in Mineral Branch, Tar Creek, and pond waters. On a given sampling day, Mineral Branch pH increases downstream; calcium, zinc, and cadmium concentrations decrease downstream; and alkalinity increases or remains constant downstream. These trends are observed for all sampling trips but are shown for only one trip. No trends are observed from the limited lead data.

There are distinct chemical differences between the Tar Creek waters in contact with low- and high-iron sediments (Figure 3). The high-iron sediments result from apparent drainage from a flooded, collapsed mine shaft at Tar Creek site 7 off the main stream. Tar Creek waters contacting low-iron sediments in the upper part of the stream are chemically similar to the Mineral Branch waters. They have higher pH and lower calcium and zinc concentrations than the waters contacting the high-iron sediments in the lower part of Tar Creek. At all Tar Creek sites, the range in alkalinity is similar. About 70−90% of the water samples have cadmium and lead concentrations below the analytical detection limit.

Water composition of a small pond (site 3) within the Mineral Branch tailings is distinct from the Mineral Branch stream chemistry. The waters are more acid (pH ~6), have lower alkalinity and calcium concentrations, and have a greater range of zinc and cadmium concentrations. The highest zinc and cadmium concentrations are about 10 times higher in the pond waters than in the stream channel. The lead concentrations are similar in the Mineral Branch pond waters and streamwaters. In the Tar Creek study area, the composition of the pond waters and streamwaters contacting the low-iron sediments are similar. Elevated calcium, zinc, cadmium, and lead concentrations are not observed in the flooded mine, despite its pH 4 waters.

We summarize the aqueous geochemistry of Mineral Branch and Tar Creek as plots of mineral saturation versus pH (Figures 5 and 6). The thermodynamic saturation index (SI) for a solid phase is equal to the ratio of its ion activity product (IAP) and its equilibrium solubility constant (K_{sp}):

$$\mathrm{SI} = \frac{\mathrm{IAP}}{K_{sp}} \qquad (1)$$

A solution is supersaturated, undersaturated, or at equilibrium if log SI is greater than, less than, or equal to 0, respectively.

Aqueous zinc, cadmium, and lead concentrations in Mineral Branch and Tar Creek waters are not controlled by the solubility of their carbonate, hydroxide, or sulfate phases. Metal carbonate and hydroxide log SI are strongly dependent

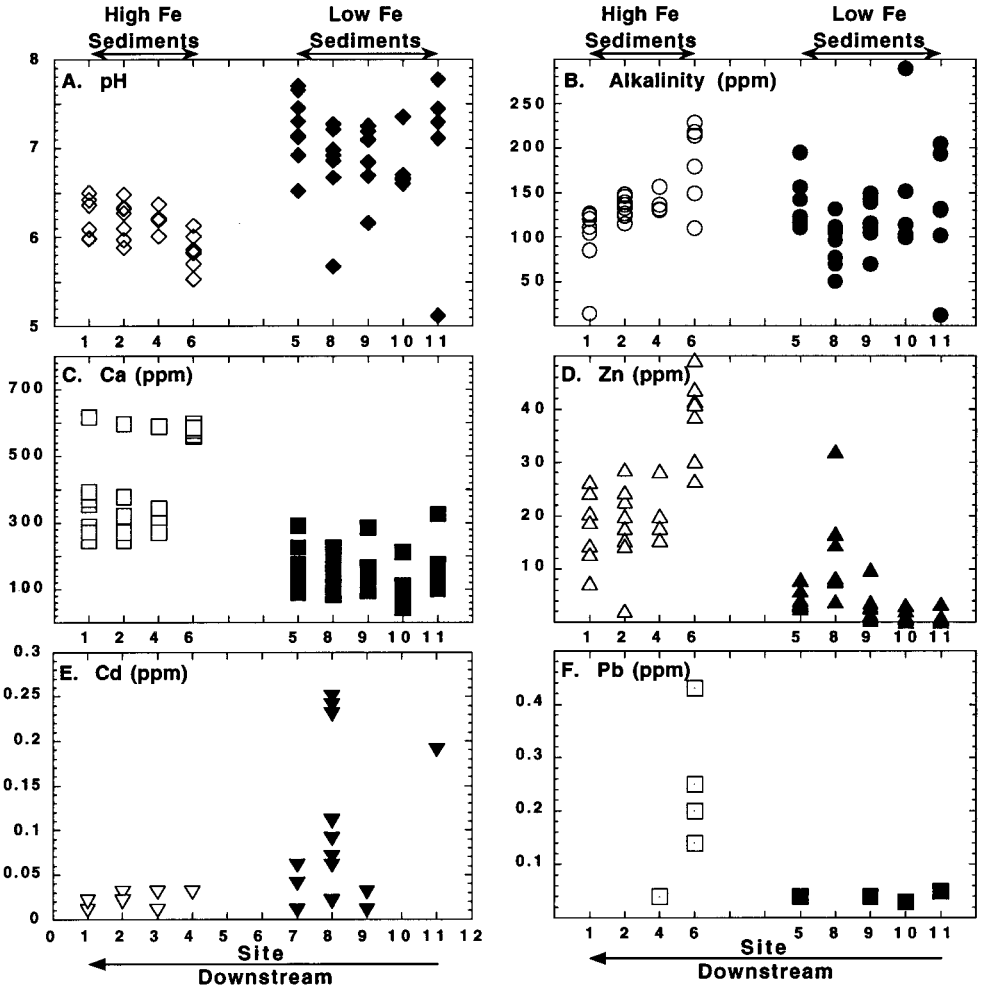

FIGURE 3. Tar Creek pH, alkalinity, and aqueous Zn, Cd, and Pb concentrations measured at each sampling site over the 1-year sampling period. Open and solid symbols represent low- and high-iron sediment, respectively.

on pH, such that the waters approach or exceed saturation with increasing pH. The waters are saturated with respect to smithsonite ($ZnCO_3$), otavite ($CdCO_3$), and cerussite ($PbCO_3$) about pH > 7 and saturated with respect to ϵ-Zn-$(OH)_2$ about pH > 8. The waters are more undersaturated with respect to hydroxide than to carbonate phases. Results for sulfate are not shown because trace metal sulfate phases are significantly more soluble than the corresponding carbonate and hydroxide phases (Table 1).

For the major elements, gypsum solubility appears to control aqueous calcium concentrations at pH < 6 (Figure 6). At pH > 6, the waters are undersaturated with respect to gypsum by as much as 3 orders of magnitude. The large scatter is probably due to charge balance calculations used to estimate sulfate concentrations. The waters are undersaturated with respect to calcite at pH < 7 and supersaturated with respect to calcite at pH > 7. Aqueous silica concentrations are controlled by quartz solubility. It is not possible to determine whether aqueous iron is controlled by the solubility of an iron oxyhydroxide because measured concentrations are below or near the analytical detection limit.

Sediment Geochemistry. The concentrations of zinc, cadmium, and lead in the sediments are much higher than the aqueous concentrations. In the Mineral Branch study area, the average zinc and lead solid-to-water ratios are both about 40 000:1; the average cadmium solid-to-water ratio is greater than 4 000:1. In the Tar Creek study area, the average zinc, cadmium, and lead solid-to-water ratios are all greater than 10 000:1. No trends in trace metal concentration or mineralogy were observed as a function of grain size.

The coordination of zinc, cadmium, and lead was identified at the molecular level in primary and secondary phases in the steam sediments by O'Day et al. (*1*) using synchrotron X-ray absorption spectroscopy. Saturation indices for coexisting waters are shown in Figures 5 and 6. In general, as sphalerite and galena weather in the stream sediments, metal coordination in secondary phases differs depending on the total iron concentration in the sediments and on pH. In low-iron sediments from Mineral Branch and upper Tar Creek, zinc appears to be taken up by zinc hydroxide and/or zinc−iron oxyhydroxide, while some cadmium and lead are associated with carbonate phases. In high-iron sediments, zinc is associated with iron oxyhydroxide, probably bonding as a bidentate inner-sphere complex to iron-octahedra, but cadmium is not found in secondary phases. In none of the samples is zinc associated with carbonate, silicate, or sulfate phases.

Discussion

We have shown that there is active exchange of the trace metals between the surface waters and the stream sediments in the U.S. Tri-State Mining District. It is the exchange of these trace metals between waters and sediments that make them a long-term hazard, both within the mining area and downstream, because dissolved trace metals are more bioavailable and thus more toxic. Figure 7 summarizes the effect of iron and carbonate chemistry on trace metal uptake and release by iron oxyhydroxide and carbonate phases and sulfide dissolution. The important geochemical processes are the competition of zinc, cadmium, and lead for iron

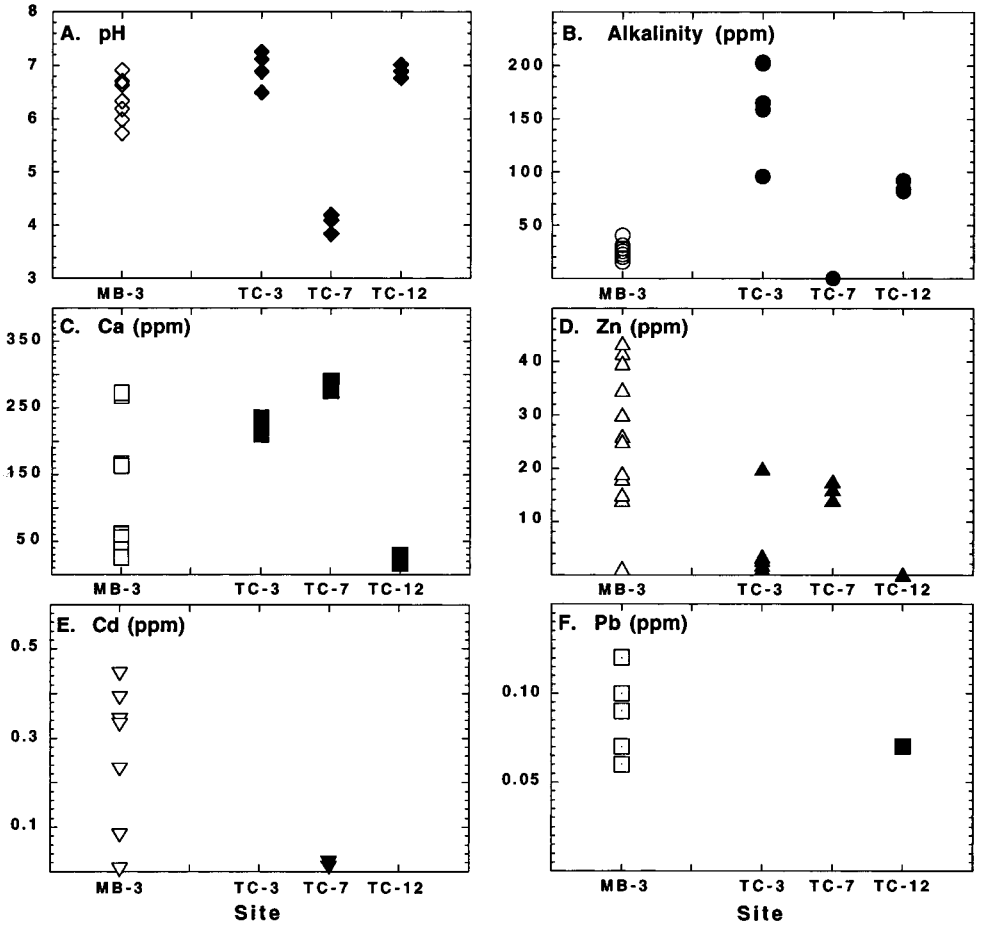

FIGURE 4. Nonstream pH, alkalinity, and aqueous Zn, Cd, and Pb concentrations in the Mineral Branch (MB, open symbols) and Tar Creek (TC, solid symbols) study areas.

oxyhydroxide and carbonate phases; degassing of $CO_2(g)$ waters and change in pH; and catalysis of sphalerite and galena dissolution by dissolved iron in near-neutral waters. These processes are discussed in detail below.

Trace Metal Uptake By Iron Oxyhydroxide and Carbonate. The XAS data (*1*) indicate that the important phases for zinc, cadmium, and lead uptake in the near-neutral U.S. Tri-State Mining District surface waters are amorphous or poorly crystalline iron oxyhydroxides and carbonates (calcite or dolomite), even though quartz is the most abundant mineral at all the low-iron sediment sample sites. In this section, we present field and laboratory evidence to illustrate the importance of accurately identifying competition among multiple metals and among multiple solid phases in complex natural systems.

Field and laboratory results indicate that zinc uptake by iron oxyhydroxide prevents cadmium uptake by this phase, making cadmium the most mobile trace metal in these waters. XAS data for Mineral Branch and Tar Creek sediments (*1*) show uptake of zinc by zinc−iron oxyhydroxides but no uptake of cadmium by these phases in the same sample. Sorption of zinc does not appear to prevent lead sorption to iron oxyhydroxides in the high-iron sediments. XAS shows Pb−O coordination at multiple distances, which is consistent with iron oxyhydroxide phases being a potential sink for lead (*1*). In laboratory experiments, Benjamin and Leckie (*14, 15*) found that zinc and lead sorption to iron oxyhydroxide suppresses cadmium sorption and that lead sorption does not interfere with zinc sorption to iron oxyhydroxides.

Our field results indicate that single solid phase experiments cannot be easily scaled to complex natural systems. In the field, we observe competition among multiple solid phases for zinc, cadmium, and lead sorption. Amorphous iron oxyhydroxide and goethite out-compete carbonate and silicate phases for zinc. This occurs even in mostly quartz sediments with about equal proportions of minor amounts of iron oxyhydroxide and calcite and in waters saturated with respect to pure zinc carbonate phases and with respect to quartz. In agreement with our results, laboratory studies have shown that iron oxyhydroxide phases effectively sorb zinc from solutions undersaturated with respect to pure zinc hydroxide phases (*15*−*19*). However in iron-free systems, zinc is associated with carbonate and silicate phases. Zachara et al. (*20, 21*) observed that zinc sorption is limited to 10% of calcite surface sites and that smithsonite ($ZnCO_3$) and hydrozincite ($Zn_5(OH)_6(CO_3)_2$) do not precipitate from solutions undersaturated with respect to these phases even in the presence of calcite. Tiller and Pickering (*22*) observed that 2:1 layered zinc silicate and hydrozincite formed from solutions slightly supersaturated with respect to quartz (2×10^{-3} M) after 1 year.

In contrast to zinc, the uptake of cadmium from solution appears to be very sensitive to otavite ($CdCO_3$) and calcite solubility. O'Day et al. (*1*) observe that cadmium substitutes in calcite in a sediment sample (TC25E) collected from pH 7.2 waters slightly supersaturated with respect to otavite and calcite but not in a chemically similar sediment sample (TC95E) collected from pH 6.8 waters slightly undersaturated with respect to otavite and calcite (Figure 5). Laboratory studies are consistent with the field observations. Stipp et al. (*23*) show that cadmium rapidly diffuses into calcite from otavite overgrowths. Other laboratory studies show that cadmium is sorbed by calcite from solutions undersaturated with respect to otavite (*24*−*29*), but they use an otavite

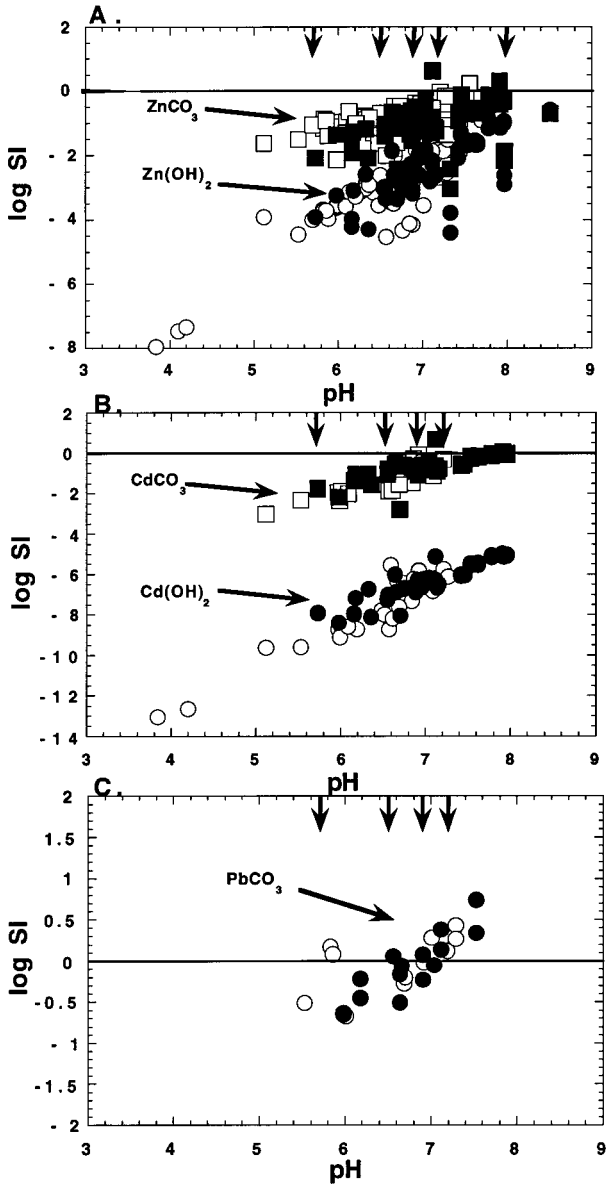

FIGURE 5. Tar Creek (open symbols) and Mineral Branch (solid symbols) solution chemistry plotted as the log SI with respect to (A) $ZnCO_3$ (squares) and ϵ-$Zn(OH)_2$ (circles); (B) $CdCO_3$ (squares) and $Cd(OH)_2$ (circles); and (C) $PbCO_3$ (circles) solubility as a function of pH. Arrows indicate sediment XAS analyses (*1*).

solubility constant that is about 2 orders of magnitude higher than the recent re-determination used in our calculations (*30*).

Uptake of lead is also distinct from zinc and cadmium. The XAS results show Pb−O coordination at multiple distances, which is consistent with both carbonate and iron oxyhydroxide phases being potential sinks for lead (*1*). Although inconclusive, these results are consistent with the low solubility of pure $PbCO_3$ (Table 1), the formation of a disordered $PbCO_3$ phase at the calcite−solution interface (*31*), and complete lead sorption at pH > 5.5 (2). When significant amounts of iron oxyhydroxide are present, sorption of lead might be expected at pH < 7, whereas competition between sorption onto iron oxyhydroxide and precipitation of carbonate phases might be expected at higher pH.

We have not modeled the field results with surface complexation and/or ion exchange models for the following reasons. (a) It is difficult to estimate the reactive surface area and the number of reactive sites for metal uptake in

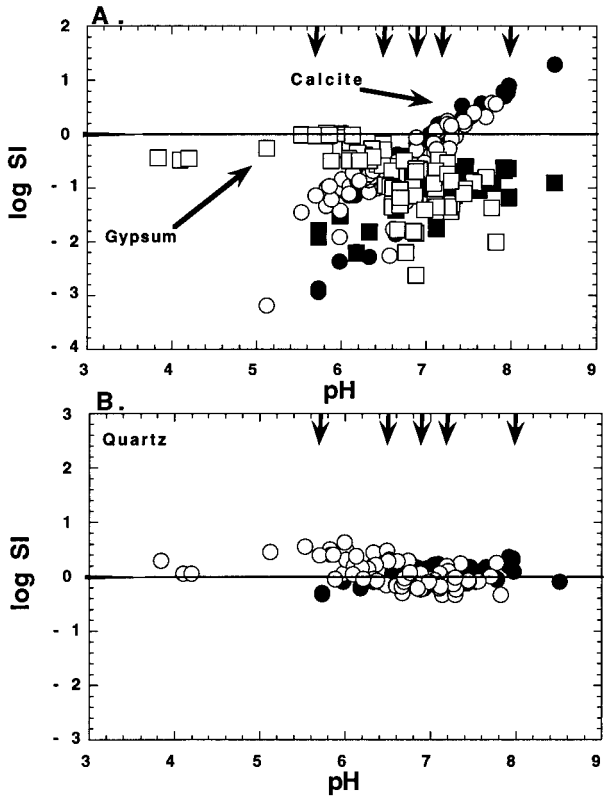

FIGURE 6. Tar Creek (open symbols) and Mineral Branch (solid symbols) solution chemistry plotted as the log SI with respect to (A) calcite (circles) and gypsum (squares) and (B) quartz as a function of pH. Arrows indicate sediment XAS analyses (*1*).

natural systems. Total surface area measurements cannot be used because metals may sorb to calcite and iron oxyhydroxide coatings on large sediments. Estimation of reactive sites from major element concentrations, such as calcium or iron, cannot be used because sediments contain multiple phases with the same elements, such as dolomite and calcite or iron oxyhydroxide and pyrite. (b) Trace metal partitioning between waters and sediments in mine drainage is a dynamic process, where sulfide dissolution kinetics provide a large, time-dependent reservoir of dissolved metals that may form secondary phases. Surface complexation and ion exchange constants are derived from static batch experiments with a limited amount of metal available for uptake. (c) These models do not consider competition among multiple solid phases for multiple metals.

Degassing of CO_2(g)-Rich Groundwater. Secondary phases are both the sink and source of zinc, cadmium, and lead as pH fluctuates. The range of pH in waters contacting the low-iron sediments is primarily from the degassing of CO_2(g)-rich waters from the underlying, unconfined carbonate aquifer that feeds the streams. This process explains the pH dependence of calcite and zinc, cadmium, and lead carbonate and hydroxide saturation indices (Figures 5 and 6). The pH increases as the waters equilibrate with atmospheric CO_2(g) and mineral solubility decreases.

The degassing of CO_2(g)-rich waters is illustrated by the increase in Mineral Branch pH along the length of the stream, from the spring source (site 5) to Center Creek (site 1) (Figure 2). In the absence of dissolution or precipitation of carbonate phases:

$$CaCO_3(\text{calcite}) + H^+ \leftrightarrow Ca^{2+} + HCO_3^- \qquad (2)$$

Alkalinity is a conservative parameter and does not change

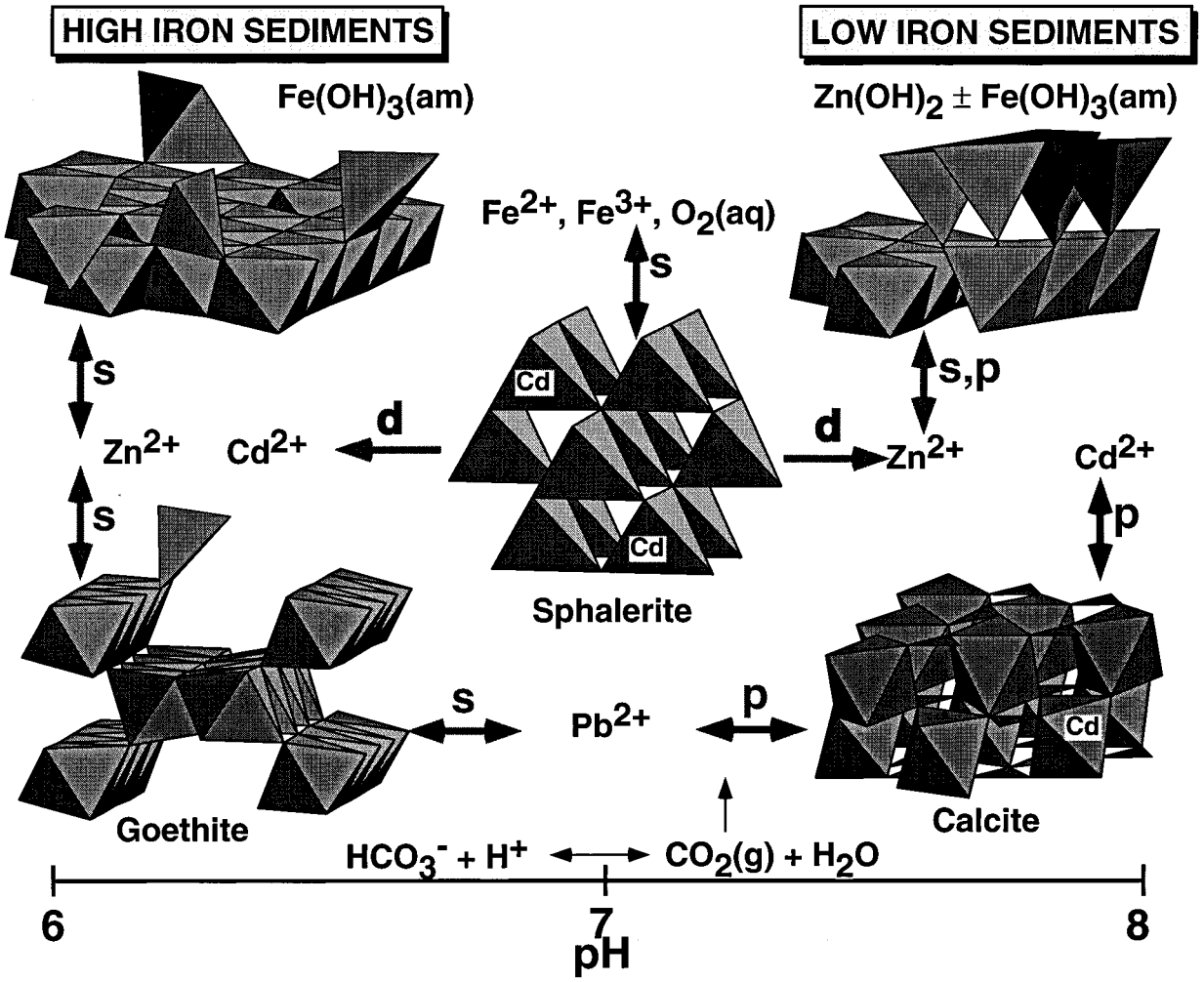

FIGURE 7. Summary of the principle rock−water interactions that control Zn, Cd, and Pb uptake in the U.S. Tri-State Mining District surface waters, where d, s, and p represent dissolution, sorption, and precipitation reactions, respectively (see text and ref 1).

as a function of pH or $pCO_2(g)$:

$$HCO_3^- + H^+ \leftrightarrow H_2O + CO_2(g) \quad (3)$$

A decrease in solution pH results in an increase in $pCO_2(g)$.

$$K = 10^{7.81}(25\ °C) = \frac{pCO_2}{\{H^+\}\{HCO_3^-\}} \quad (4)$$

Two types of waters are indicated by the linear trends in log $pCO_2(g)$ versus pH for Mineral Branch and Tar Creek samples (Figure 8). Most of the data fall on the upper trend and can be explained by the degassing of $CO_2(g)$-rich waters as they equilibrate with atmospheric $CO_2(g)$. The decrease in calcium observed in the Mineral Branch waters (Figure 2) corresponds to a 3−10% change in the measured alkalinity. The lower trend represents interaction of oxygen-rich, meteoric waters with the residual sulfides and calcite in the tailings piles (Mineral Branch site 3), which have much lower alkalinity and calcium concentrations than the streamwaters.

Sulfide Dissolution Kinetics. Iron chemistry may directly effect the solubility of metals by increasing the dissolution rate of sulfide minerals present in the sediments. Rimstidt et al. (*32*) found that Fe(III) accelerates sphalerite and galena dissolution in acid solutions. In near-neutral solutions similar to the Tri-State surface waters, both dissolved oxygen and iron have been reported to accelerate pyrite dissolution (*33*−*37*). Moses and Herman (*36*) propose that Fe(II) sorbs

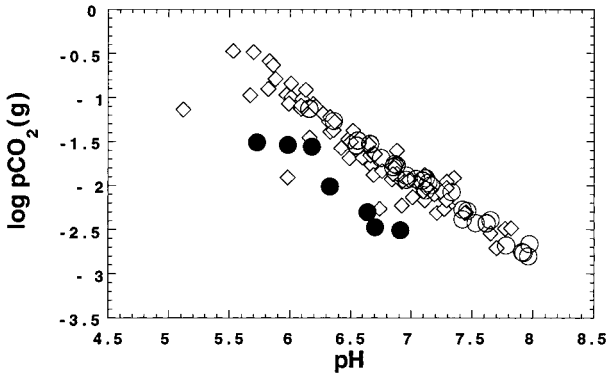

FIGURE 8. Log $pCO_2(g)$ versus pH for Tar Creek waters (open diamonds) and Mineral Branch sites 1, 2, 4, and 5 (open circles) and Mineral Branch site 3 (solid circles).

to a sulfur site on the pyrite surface and is then oxidized to Fe(III) by dissolved oxygen. The electron is then transferred to sulfur, and Fe(III) is reduced to Fe(II). This process repeats itself until enough electrons have been transferred to oxidize sulfur and to dissolve pyrite. It is probable that a similar electron transfer occurs between sulfur sites, sorbed iron, and dissolved oxygen to accelerate sphalerite and galena dissolution in near-neutral waters. Microbial catalysis is another important process; however, it is expected to be minimal in this system because sulfide oxidizing bacteria do not thrive above pH 4 (*38*).

The higher aqueous zinc and cadmium concentrations and more acid pH (~6) in the small pond near Mineral Branch (site 3) than in the nearby stream may be explained by the oxidation of sphalerite by dissolved iron (Figures 2 and 3). Acidity normally associated with mine drainage is caused by the oxidation of iron sulfide, such as pyrite, by dissolved oxygen

$$FeS_2 + 7/2O_2(g) + H_2O \leftrightarrow Fe^{2+} + 2SO_4^{2-} + 2H^+ \quad (5)$$

or by Fe(III)

$$FeS_2 + 14Fe^{3+} + 8H_2O \leftrightarrow 2SO_4^{2-} + 15Fe^{2+} + 16H^+ \quad (6)$$

and by the precipitation of iron oxyhydroxide

$$Fe^{2+} + 1/4O_2(g) + 3/2H_2O \leftrightarrow FeOOH + 3H^+ \quad (7)$$

However, sphalerite oxidation must involve reduction of Fe(III) to increase acidity:

$$ZnS + 8Fe^{3+} + 4H_2O \leftrightarrow Zn^{2+} + SO_4^{2-} + 8Fe^{2+} + 8H^+ \quad (8)$$

No acidity is produced from sphalerite oxidation by dissolved oxygen alone:

$$ZnS + 2O_2(g) \leftrightarrow Zn^{2+} + SO_4^{2-} \quad (9)$$

Another possible explanation for the observed increase in acidity and zinc and cadmium concentrations is sphalerite and pyrite dissolution by dissolved oxygen and precipitation of iron oxyhydroxides without the uptake of zinc in a secondary phase. This interpretation is based on the lack of elevated aqueous iron in these waters. However, it seems unlikely that secondary iron-oxyhydroxides would not rapidly remove zinc from solution.

The high aqueous zinc concentrations in contact with the high iron sediments (Figure 3) is consistent with a positive feedback mechanism between iron chemistry and sulfide dissolution. The source for the abundance of iron oxyhydroxide downstream of the confluence of Lytle and Tar Creek is likely to be pyrite. Pyrite oxidization by Fe(III) (eq 6) would increase dissolved iron, which would accelerate both pyrite and sphalerite dissolution (eq 8) and decrease pH. Precipitation or coprecipitation of iron oxyhydroxide (eq 7) and zinc hydroxide would also decrease pH

$$Zn^{2+} + 2H_2O \leftrightarrow Zn(OH)_2 + 2H^+ \quad (10)$$

A decrease in pH would desorb zinc from iron oxyhydroxide leading, to an increase in aqueous zinc (*2*).

The lead field data also point to the possible involvement of iron oxidation of sulfide minerals. The lack of galena in the sediments may indicate that galena dissolution is faster than sphalerite dissolution. Sediment zinc concentrations are about 10 times sediment lead concentrations. Galena dissolution rates would need to be five times sphalerite dissolution rates to dissolve all the galena and half the sphalerite, assuming that aqueous zinc and lead are effectively scavenged by secondary phases. At pH 7 in the absence of Fe(III), PbS dissolution rates (*39*) are similar to sphalerite dissolution rates (*35*). However, Rimstidt et al. (*32*) measured PbS dissolution rates that are 300 times faster than ZnS dissolution rates at pH 2 by monitoring the reduction of Fe(III) to Fe(II).

The dissolution of cadmium from sphalerite in the stream sediments is consistent with laboratory studies. In the high-iron sediments (pH ~6), the XAS results show that cadmium has the same structural environment as in fresh Tri-State sphalerite ore. However, in one of the low-iron sediments (pH ~7), the XAS results show disorder around cadmium and order around zinc in residual sphalerite. This may suggest that localized CdS domains in sphalerite are being leached at a greater rate than the bulk ZnS. Laboratory studies at pH 7 show that short-term (<6 h) CdS dissolution rates (*40, 41*) are about an order of magnitude faster than ZnS dissolution rates (*35*). Additionally, Hsieh (*41*) show that, under photoirradiation and aerobic conditions, aqueous zinc exchanges for cadmium at the CdS surface, increasing CdS dissolution.

The surface waters draining the U.S. Tri-State Mining District achieve chemical steady state, but they are not at thermodynamic equilibrium. Degassing of CO_2(g)-rich waters and the resulting changes in pH drive carbonate and hydroxide dissolution and precipitation reactions. There is significant evidence of trace metal uptake on secondary phases, but equilibrium cannot be obtained because pCO_2-(g) and pH are not constant. The importance of CO_2(g) to aqueous trace metals concentrations can be seen in the range of pH and zinc and cadmium concentrations measured in the streamwaters over the 1-year sample period (Figures 2−4). The impact of pH on water quality can be seen by comparing the increase in aqueous zinc concentration in Tar Creek below its intersection with Lytle Creek. Low-iron sediments are transported from average pH 7 waters in the upper part of Tar Creek to average pH 6 waters in the lower part of Tar Creek. When these sediments react with the more acid waters and the high-iron sediments, zinc desorbs or dissolves (Figure 3). This process may occur concurrently with catalysis of sphalerite dissolution by Fe(III), which may also increase aqueous zinc concentration.

Acknowledgments

S.A.C. acknowledges support from the Institute of Geophysics and Planetary Physics and the Laboratory Directed Research and Development Program under the auspices of Department of Energy Contract W-9405-ENG-48. P.A.O. acknowledges support from the Arizona State University Faculty Grant-In-Aid Program. S.A.C. and M.F.P. acknowledge support from University of Missouri Weldon Spring Fund and United States Department of Interior, Geological Survey; J. Johnson for revising the thermodynamic database; and G. Mehlhose for collection and preparation of field samples.

Literature Cited

(1) O'Day, P. A.; Carroll, S. A.; Waychunas, G. A. *Environ. Sci. Technol.* **1998**, *32*, 943−955.
(2) Dzombak, D. A.; Morel, F. M. M. *Surface Complexation Modeling*; John Wiley & Sons: New York, 1990; p 393.
(3) Zachara, J. M.; Cowan, C. E.; Resch, C. T. In *Metals in Groundwater*; Allen, H. E., Perdue, E. M., Brown, D. S., Eds.; Lewis Publishers: Chelsea, MI, 1993; pp 37−71.
(4) Charlet, L.; Manceau, A. In *Environmental Particles*; Buffle J., Van Leeuwen H. P., Eds.; Lewis Publishers: Chelsea, MI, 1993; pp 117−164.
(5) Brown, G. E., Jr.; Parks, G. A.; O'Day, P. A. In *Mineral Surfaces*; Vaughan, D. J., Pattrick, R. A. D., Eds.; Chapman & Hall: London, 1995; pp 129−183.
(6) Brockie, D. C.; Hare, E. H.; Dingess, P. R. In *Ore Deposits of the United States, 1933−1967*; Ridge, J. D., Ed.; AIME: New York, 1968; pp 400−430.
(7) McKnight, E. T.; Fischer, R. P. *U.S. Geol. Surv. Prof. Pap.* **1970**, *No. 588*.
(8) Bethke, C. M. *The Geochemist's Workbench. A users guide to Rxn, Act2, TAct, React, and Gtplot*, 2nd ed.; University of Illinois: Urbana−Champaign, 1994; p 213.
(9) Johnson, J. W.; Oelkers, E. H.; Helgeson, H. C. *Comput. Geosci.* **1992**, *18*, 899.
(10) Chapman, B. M.; Jones, D. R.; Jung, R. F. *Geochim. Cosmochim. Acta* **1983**, *47*, 1957.
(11) Filipek, L. H.; Nordstrom, D. K.; Ficklin, W. *Environ. Sci. Technol.* **1987**, *21*, 388.

(12) Moore, J. N.; Ficklin, W. H.; Johns, C. *Environ. Sci. Technol.* **1988**, 22, 432.
(13) Davis, A.; Olsen, R. L.; Walker, D. R. *Appl. Geochem.* **1991**, *6*, 333.
(14) Benjamin, M. M.; Leckie J. O. In *Contaminants and Sediments*; Baker, R. A., Ed.; American Chemical Society: New York, 1980.
(15) Benjamin, M. M.; Leckie, J. O. *J. Colloid Interface Sci.* **1981**, 79, 209.
(16) Kinniburgh, D. G.; Jackson, M. L. *Soil Sci. Soc. Am. J.* **1982**, *46*, 56.
(17) Dzombak, D. A.; Morel, F. M. M. *J. Colloid Interface Sci.* **1986**, *112*, 588.
(18) Harvey, D. T.; Linton, R. W. *Colloids Surf.* **1984**, *11*, 81.
(19) Waychunas, G. A.; Fuller, C. C, Davis, J. A. *Stanford Synchrotron Radiation Laboratory Activity Report*; 1995.
(20) Zachara, J. M.; Kittrick J. A.; Harsh, J. *Geochim. Cosmochim. Acta* **1988**, *52*, 2281.
(21) Zachara, J. M.; Kittrick, J. A.; Dake, L. S.; Harsh, J. B. *Geochim. Cosmochim. Acta* **1989**, *53*, 9.
(22) Tiller, K. G.; Pickering, J. G. *Clays Clay Miner.* **1974**, *22*, 409.
(23) Stipp, S. L.; Hochella, M. F., Jr., Parks, G. A.; Leckie, J. O. *Geochim. Cosmochim. Acta* **1992**, *56*, 1941.
(24) Lorens, R. B. *Geochim. Cosmochim. Acta* **1981**, *45*, 553.
(25) Davis, J. A.; Fuller, C. C.; Cook, A. D. *Geochim. Cosmochim. Acta* **1987**, *51*, 1477.
(26) Fuller, C. C.; Davis, J. A. *Geochim. Cosmochim. Acta* **1987**, *51*, 1491.
(27) Zachara, J. M.; Cowan, C. E.; Resh, C. T. *Geochim. Cosmochim. Acta* **1991**, *55*, 1549.
(28) van der Weijden, R. D.; van der Weijden, C. H.; Comans, R. N. J. *Mar. Chem.* **1994**, *47*, 65.
(29) Bilinski, H.; Sirac, S.; Kozar, S.; Branica, M. Schwuger, M. J. *Water Res.* **1995**, *29*, 1993.
(30) Stipp, S. L. S.; Parks, G. A.; Nordstrom, D. K.; Leckie, J. O. *Geochim. Cosmochim. Acta* **1993**, *57*, 2699.
(31) Sturchio, N. C.; Chiarello, R. P.; Cheng, L.; Lynam, P. F.; Bedzyk, M. J.; Qian, Y.; You, H.; Yee, D.; Geissbuhler, P.; Sorensen, L. B.; Liang, Y.; Baer, D. R. *Geochim. Cosmochim. Acta* **1997**, *61*, 251.
(32) Rimstidt, J. D.; Chermak, J. A.; Gagen, P. M. In *Environmental Geochemistry of Sulfide Oxidation*; Alpers, C. N., Blowes, D. W., Eds.; American Chemical Society: Washington, DC, 1994; pp 2−13.
(33) Goldhaber, M. B. *Am. J. Sci.* **1983**, *283*, 193.
(34) McKibben, M. A.; Barnes, H. L. *Geochim. Cosmochim. Acta* **1986**, *50*, 1509.
(35) Moses, C. O.; Nordstrom, D. K.; Herman, J. S.; Mills, A. L. *Geochim. Cosmochim. Acta* **1987**, *51*, 1561.
(36) Moses, C. O.; Herman, J. S. *Geochim. Cosmochim. Acta* **1991**, *55*, 471.
(37) Nicholson, R. V.; Gillham, R. W.; Reardon, E. J. *Geochim. Cosmochim. Acta* **1988**, *52*, 1077.
(38) Nordstrom, D. K. In *Acid Sulfate Weathering*; Soil Science Society of America: Madison, WI, 1982; pp 37−63.
(39) Hsieh, Y. H.; Huang, C. P. J. *Colloid Interface Sci.* **1989**, *131*, 537.
(40) Hsieh, Y. H.; Huang, C. P. *Colloids Surf.* **1991**, *53*, 275.
(41) Hsieh, Y. H.; Huang, C. P.; Davis, A. P. *Chemosphere* **1992**, *24*, 281.
(42) Helgeson, H. C.; Delany, J. M.; Nesbitt, H. W.; Bird, D. K. *Am. J. Sci.* **1978**, *278-A*, 1.
(43) Robie, R. A.; Hemingway, B. S.; Fisher, J. S. *U.S. Geol. Survey Bull.* **1979**, *No. 1452*, 1.
(44) Baes, C. F. J.; Mesmer, R. E. *The Hydrolysis of Cations;* Wiley-Interscience: New York, 1976; p 489.
(45) Wagman, D. D.; Evans, W. H.; Parker, V. B.; Schumm, R. H.; Halow, I.; Bailey, S. M.; Churney, K. L.; Nuttall, R. L. *J. Phys. Chem. Ref. Data* **1982**, *11* (Suppl. 2).
(46) Cox, J. D.; Wagman, D. D.; Medvedev, V. A. *CODATA Key Values for Thermodynmics*; Hemisphere: Bristol, PA, 1989.
(47) Smith, R. M.; Martell, A. E. *Critical Stability Constants*, 2nd ed.; Plenum Press: New York, 1989, Vol. 4, p 256.
(48) Bilinski, H.; Schindler, P. *Geochim. Cosmochim. Acta* **1982**, *46*, 921.
(49) Bourcier, W. L.; Barnes, H. L. *Econ. Geol.* **1987**, *82*, 1839.
(50) Schindler, P.; Reinert; M.; Gamsjäger, H. *Helv. Chim. Acta* **1969**, *52*, 2327.

Received for review May 23, 1997. Revised manuscript received October 30, 1997. Accepted January 20, 1998.

ES970452K